Vacancy-Induced Low-Energy States in Undoped Graphene

Sambuddha Sanyal,[1] Kedar Damle,[2] and Olexei I. Motrunich[3]

[1]*International Center for Theoretical Sciences, Tata Institute of Fundamental Research, Bengaluru 560089, India*
[2]*Department of Theoretical Physics, Tata Institute of Fundamental Research, Mumbai 400005, India*
[3]*Department of Physics, California Institute of Technology, Pasadena, California 91125, USA*
(Received 2 September 2015; published 9 September 2016)

We demonstrate that a nonzero concentration n_v of static, randomly placed vacancies in graphene leads to a density w of zero-energy quasiparticle states at the band center $\epsilon = 0$ within a tight-binding description with nearest-neighbor hopping t on the honeycomb lattice. We show that w remains generically nonzero in the compensated case (exactly equal number of vacancies on the two sublattices) even in the presence of hopping disorder and depends sensitively on n_v and correlations between vacancy positions. For low, but not-too-low, $|\epsilon|/t$ in this compensated case, we show that the density of states $\rho(\epsilon)$ exhibits a strong divergence of the form $\rho_{\mathrm{Dyson}}(\epsilon) \sim |\epsilon|^{-1}/[\log(t/|\epsilon|)]^{(y+1)}$, which crosses over to the universal low-energy asymptotic form (modified Gade-Wegner scaling) expected on symmetry grounds $\rho_{\mathrm{GW}}(\epsilon) \sim |\epsilon|^{-1}e^{-b[\log(t/|\epsilon|)]^{2/3}}$ below a crossover scale $\epsilon_c \ll t$. ϵ_c is found to decrease rapidly with decreasing n_v, while y decreases much more slowly.

Static impurities, which give rise to random time-independent terms in the single-particle Hamiltonian for quasiparticle excitations of a condensed matter system, can lead to the phenomenon of Anderson localization, whereby quasiparticle wave functions lose their plane-wave character and become localized [1]. Such localization transitions and universal low-energy properties of the localized phase have been successfully described in many cases using effective field theories [2,3] whose form depends on symmetry properties of the quasiparticle Hamiltonian in the presence of impurities. In some cases [4,5], it has also been possible to refine these field-theoretical predictions using real-space strong-disorder renormalization group ideas [6].

In this Letter, we study the effects of a nonzero concentration n_v of static, randomly located vacancies in graphene. We use a tight-binding description for electronic states of graphene, with hopping amplitude t between nearest-neighbor sites on a honeycomb lattice, and model vacancies by the deletion of the corresponding site in this tight-binding model [7–11]. We focus on the compensated case, i.e., exactly equal numbers of vacancies on the two sublattices of the honeycomb lattice, and demonstrate that vacancies generically lead to a nonuniversal density w of zero-energy quasiparticle states at the band center $\epsilon = 0$ even in this compensated case, including in the presence of hopping disorder. For low, but not-too-low, $|\epsilon|/t$ in this compensated case, the density of states (DOS) $\rho(\epsilon)$ exhibits a strong divergence of the form

$$\rho_{\mathrm{Dyson}}(\epsilon) \sim |\epsilon|^{-1}/[\log(t/|\epsilon|)]^{(y+1)}, \qquad (1)$$

familiar in the context of various random-hopping problems in one dimension [12–20]. At still lower energies,

below a crossover scale ϵ_c that is several orders of magnitude smaller than t even for moderately small values of n_v (0.05–0.1), we show that the DOS crosses over to the low-energy asymptotic behavior [4–6,21] of the chiral orthogonal universality class (to which our tight-binding model belongs on symmetry grounds):

$$\rho_{\mathrm{GW}}(\epsilon) \sim |\epsilon|^{-1}e^{-b[\log(t/|\epsilon|)]^{2/3}}. \qquad (2)$$

The density of zero-energy states w depends sensitively on correlations between vacancies and decreases as n_v is lowered. The crossover energy ϵ_c is found to decrease rapidly with decreasing w, while y [in fits to Eq. (1) for $|\epsilon| > \epsilon_c$] decreases much more slowly. On comparing the corresponding crossover length scale l_c, defined as the mean spatial separation between nonzero-energy modes with $|\epsilon| < \epsilon_c$, with $l_w \equiv w^{-1/2}$, the mean spatial separation between zero-energy states, we find that l_c tracks l_w up to a nonuniversal prefactor. Thus, our results imply that the $w \to 0$ limit of the DOS is singular and does not commute with the $\epsilon \to 0$ limit: For any $w > 0$, the true asymptotic form $\rho_{\mathrm{GW}}(\epsilon)$ cannot be obtained from an extrapolation of results obtained for $\epsilon_c < \epsilon \ll t$, which instead reflect the intermediate-energy physics encoded in the form $\rho_{\mathrm{Dyson}}(\epsilon)$.

Our work sheds light on an interesting question motivated by the results of Willans *et al.*, who found a vacancy-induced DOS of the form $\rho_{\mathrm{Dyson}}(\epsilon)$ at not-too-low energies in their study of Majorana excitations of Kitaev's honeycomb model [22]: Does a nonzero vacancy density lead to a low-energy limit that is qualitatively different from the asymptotic behavior expected in the chiral orthogonal universality class of quasiparticle localization? In recent work that addressed this question in the context of graphene

[23], it was argued that vacancies lead to a new term in the low-energy field theory, which causes the DOS to take on the form $\rho_{\text{Dyson}}(\epsilon)$ [Eq. (1)], with $y = 1/2$ at asymptotically low energies, rather than the asymptotic form $\rho_{\text{GW}}(\epsilon)$ [Eq. (2)] expected on symmetry grounds. In parallel work [24], this prediction was found to be consistent with numerical results for the DOS.

While we do find that the DOS fits well to $\rho_{\text{Dyson}}(\epsilon)$ at intermediate energies ($\epsilon_c \ll \epsilon \ll t$), albeit with a nonuniversal y, our conclusion regarding the asymptotic low-energy behavior is clearly very different and raises two perhaps more interesting questions: When $\epsilon_c \ll t$, are the crossover exponent y and crossover energy ϵ_c "universally" determined by the zero-mode density w, although the function $w(n_v)$ itself depends sensitively on microscopic details such as correlations between vacancies? Can this crossover be understood within a renormalization group description of the low-energy physics, perhaps using the ideas of Ref. [23]? Leaving these interesting questions for future work, we devote the remainder of this Letter to an account of the calculations that lead us to our results, and thence, to these questions.

We choose the lattice spacing of the honeycomb lattice as our unit of length and measure all energies in terms of the hopping amplitude t, which is set by the bandwidth of the π band of undoped graphene. We focus on the compensated case, with exactly $n_v L^2$ vacancies placed randomly on each sublattice of a finite $L \times L$ honeycomb lattice with L^2 unit cells ($2L^2$ sites). The spectrum of single-particle states can be obtained by diagonalizing the real symmetric matrix H

$$H = \begin{pmatrix} 0 & T_{AB} \\ T_{AB}^\dagger & 0 \end{pmatrix}, \tag{3}$$

where T_{AB} is the $(1 - n_v)L^2$-dimensional matrix of amplitudes for hopping from the undeleted sites of the B sublattice to their undeleted A-sublattice neighbors and $T_{AB}^\dagger$ is the transpose of this matrix (the spin label of the electronic quasiparticles is dropped since we do not study magnetic properties or sources of spin-flip scattering in this Letter).

The purely off-block-diagonal form of H reflects the "chiral" symmetry of the problem, corresponding to the bipartite structure of the honeycomb lattice, which guarantees that every eigenstate with energy $\epsilon > 0$ has a corresponding eigenstate at energy $-\epsilon$. In order to eliminate zero modes of H in the pure $L \times L$ lattice [25–27], we choose even values of L and impose antiperiodic boundary conditions along the $\hat{x}$ direction, while terminating the lattice in the $\hat{y}$ direction in a pair of armchair edges. We also impose a nearest-neighbor and next-nearest-neighbor exclusion constraint on the vacancies and do not allow them to interrupt the armchair edges. These restrictions, along with the compensated nature of the vacancy disorder, eliminate all previously studied and well-understood sources of vacancy-induced [9,28] zero modes in the spectrum of H.

We find it convenient to focus on the symmetric matrix $T_{AB}^\dagger T_{AB}$, which has a single eigenvalue ϵ^2 for every pair of nonzero eigenvalues ($\epsilon, -\epsilon$) of H. Zero modes of $T_{AB}^\dagger T_{AB}$, with wave functions living entirely on the B sublattice, map on to exactly half of the zero modes in the spectrum of H, while zero modes of the symmetric matrix $T_{AB} T_{AB}^\dagger$, with wave functions living entirely on the A sublattice, make up the other half of the null space of H. We use the ALGOL [29] routines of Martin and Wilkinson [30] to compute the number $\mathcal{N}_\Lambda$ of eigenvalues of the banded matrix $T_{AB}^\dagger T_{AB}$, which are smaller in magnitude than some positive number $t^2 \times 10^{-\Lambda}$. Our implementation [31] uses calls to the GNU multiprecision library [32] for all arithmetic operations, including comparison of the magnitudes of two numbers, and has been benchmarked against routines from the LAPACK library [33] as well as C translations (used in earlier work [6]) of the ALGOL routines of Martin and Wilkinson.

Anticipating that the physics of interest to us spans many orders of magnitude in energy ϵ, we define the log energy $\Gamma = \log_{10}(t/|\epsilon|)$ and compute $N_{\text{tot}}^{(i)}(\Gamma, L) \equiv \mathcal{N}_{\Lambda = 2\Gamma}^{(i)}/L^2$ for the ith $L \times L$ random sample using values of log energy drawn from an equispaced grid ranging from $\Gamma \sim 1$ to $\Gamma \sim 100$. For large enough Γ, $N_{\text{tot}}^{(i)}(\Gamma, L)$ plateaus out to a constant value that represents the density of zero modes $w_L^{(i)}$ of that sample. For not-too-small n_v ($n_v \geq 0.05$) for which we are able to access this plateau, we separately keep track of $w_L^{(i)}$ and $N_L^{(i)}(\Gamma) \equiv N_{\text{tot}}^{(i)}(\Gamma, L) - w_L^{(i)}$. From the position $\Gamma_g^{(i)}(L)$ of the last downward step in $N_{\text{tot}}^{(i)}(\Gamma, L)$, we also obtain the spectral gap $\epsilon_g^{(i)}(L) \equiv t \times 10^{-\Gamma_g^{(i)}(L)}$ corresponding to the lowest pair of nonzero eigenvalues $\pm \epsilon_g^{(i)}$ for that sample. Analyzing this data for up to 3000 samples for each value of L and n_v, we obtain statistically reliable estimates of the corresponding disorder-averaged quantities w_L and $N_L(\Gamma)$. The density of states $\rho_L(\epsilon)$ can then be obtained from N_L using the relation $\rho_L(\epsilon) \equiv (1/2\epsilon)dN_L/d\Gamma$. Additionally, we estimate f_L, the probability that an $L \times L$ sample has at least one pair of zero modes, and measure the histogram of $\Gamma_g(L)$. The position of the peak in the latter provides us an estimate of $\Gamma_g^*(L)$, the most probable value of $\Gamma_g(L)$. For the smallest values of n_v, which require multiprecision computation at impracticably large Γ in order to access the plateau in $N_{\text{tot}}^{(i)}(\Gamma, L)$ (and thence $w_L^{(i)}$), we instead compute $dN_L/d\Gamma$ by numerical differentiation of $N_{\text{tot}}^{(i)}(\Gamma, L)$.

Extrapolating our results for f_L (see the Supplemental Material [34]) and w_L (Fig. 1) to obtain $f \equiv \lim_{L \to \infty} f_L$ and $w \equiv \lim_{L \to \infty} w_L$, we find that $f = 1$ and that w depends sensitively on n_v (Fig. 1). To understand these results, we observe that $T_{AB} T_{AB}^\dagger$ ($T_{AB}^\dagger T_{AB}$) must have a zero mode, with the wave function shown in Fig. 2, if four of the B-sublattice vacancies (six of the A-sublattice
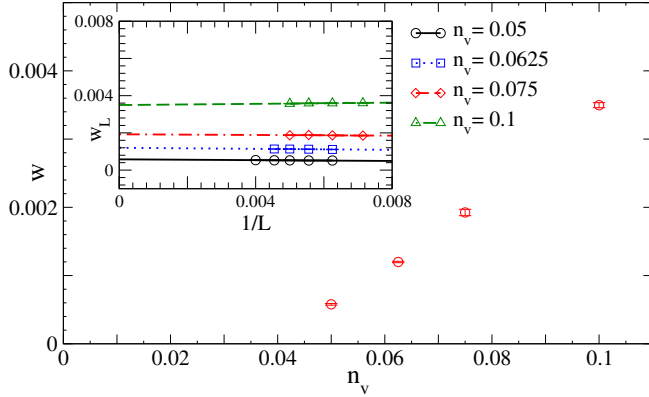
FIG. 1. w_L, the density of zero modes in an $L \times L$ sample, tends to a nonzero thermodynamic limit w that depends on n_v, the concentration of vacancies.

vacancies) are arranged in the specific four-triangle pattern ($\mathcal{R}_6$ motif) shown in Fig. 2, with no restrictions on the positions of the other vacancies. H must therefore have a pair of zero modes if a single four-triangle or $\mathcal{R}_6$ motif occurs anywhere in the sample on either sublattice. Since there is a nonzero probability of finding a four-triangle at a given location, this already implies that a large enough sample will certainly have at least one zero mode, i.e., $f = 1$. Additionally, one has an elementary lower bound on $w_L^{(i)}$ in terms of the numbers $N_{\Delta_{4A}}^{(i)}$ and $N_{\Delta_{4B}}^{(i)}$ of four-triangles on A and B lattices in a given sample: $w_L^{(i)} \geq [\max(N_{\Delta_{4A}}^{(i)}, N_{\Delta_{4B}}^{(i)})]/L^2$, implying $w \geq n_{\Delta_4}$, where n_{Δ_4} is the ensemble-averaged concentration of four-triangles in the thermodynamic limit. When the vacancies obey the exclusion constraints described earlier, it is not possible to produce a similar zero mode with fewer than
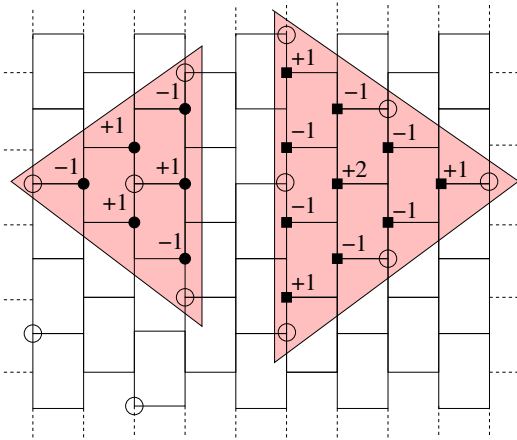

FIG. 2. Four B-sublattice (six A-sublattice) vacancies arranged in a four-triangle pattern ($\mathcal{R}_6$ motif) give rise to a zero mode of H living on A-sublattice sites (B-sublattice sites) within the four-triangle ($\mathcal{R}_6$ motif). While hopping disorder eliminates the four-triangle zero mode, it only changes the wave function of the $\mathcal{R}_6$ zero mode without changing its energy.

four vacancies (see the Supplemental Material [34]). Thus, we expect $w \sim n_v^4$ in the $n_v \to 0$ limit.

While our lower bound can be strengthened somewhat by including larger versions of the four-triangle motif (see the Supplemental Material [34]), they do not change this limiting behavior. However, our results (Fig. 1) suggest that this limiting behavior sets in only for $n_v \ll 0.05$, for which a direct computation of w would require access to impracticably large Γ. For $n_v \gtrsim 0.05$, four-triangles are not the dominant contribution to w (see the Supplemental Material [34]), which we expect arises instead from generalizations of the $\mathcal{R}_6$ motif: Such $\mathcal{R}$-type regions have more undeleted sites belonging to one sublattice than the other but are connected to the rest of the lattice only via sites belonging to the other sublattice. Like the $\mathcal{R}_6$ zero mode, all such $\mathcal{R}$-type zero modes are robust to disorder in the nearest-neighbor hopping amplitudes (see the Supplemental Material [34]). Unlike zero modes associated with specific patterns like four-triangles, these $\mathcal{R}$-type zero modes cannot be eliminated by any additional local constraints on the vacancy positions. They are therefore a generic feature of the diluted graphene lattice. Thus, we see that a nonzero concentration n_v of vacancies leads to a density w of zero modes of H, where w depends sensitively on n_v and on correlations in the positions of vacancies, but remains generically nonzero even in the compensated case, including in the presence of hopping disorder.

Figure 3 displays $N_L(\Gamma)$ for $n_v = 0.0625$ and $n_v = 0.1$ for the three largest sizes used in our extrapolations to the thermodynamic limit. Since we expect finite-size effects to dominate for $\Gamma > \Gamma_g^*(L)$, we estimate $\Gamma_g^*(L)$ from histograms of $\Gamma_g(L)$ (see the Supplemental Material [34]) and restrict attention to $\Gamma < \Gamma_g^*(L_{\min})$, where $L_{\min}$, the smallest of the sizes used in our extrapolations, is chosen large enough that $f_{L_{\min}} \approx 1$ in order to ensure that the physics of zero modes is correctly captured in all our analysis. In this range of Γ, we can reliably extrapolate (see the Supplemental Material [34]) from our data to obtain the thermodynamic limit $N(\Gamma)$ displayed in the inset of Fig. 3. Up to a fairly well-defined and readily identified crossover scale $\Gamma_c(L) \equiv \log_{10}(t/|\epsilon_c(L)|)$, $N_L(\Gamma)$ is found to fit well to a power-law form $N_{\mathrm{Dyson}}(\Gamma) \equiv c\Gamma^{-y}$. However, for larger Γ beyond Γ_c, the asymptotic falloff is clearly faster than a power law. $\Gamma_c(L)$ increases slightly with L over the range of L studied but saturates at large L to a finite thermodynamic limit Γ_c that marks the presence of the same crossover in the limiting curve $N(\Gamma)$. Thus, $N(\Gamma)$ is again fit well by the power-law form N_{Dyson} for $\Gamma \lesssim \Gamma_c$ but falls off much faster in the large-Γ regime.

Given that H belongs to the chiral orthogonal universality class, standard universality arguments predict that $N(\Gamma)$ and $N_L(\Gamma)$ should, at large enough Γ, follow the modified Gade-Wegner form [4–6,21] $N_{\mathrm{GW}}(\Gamma) \equiv a\Gamma^{1/3}e^{-b\Gamma^{2/3}}$. From Fig. 3, we see that this form indeed provides a very good fit in the asymptotic large-Γ regime. The same crossover is also
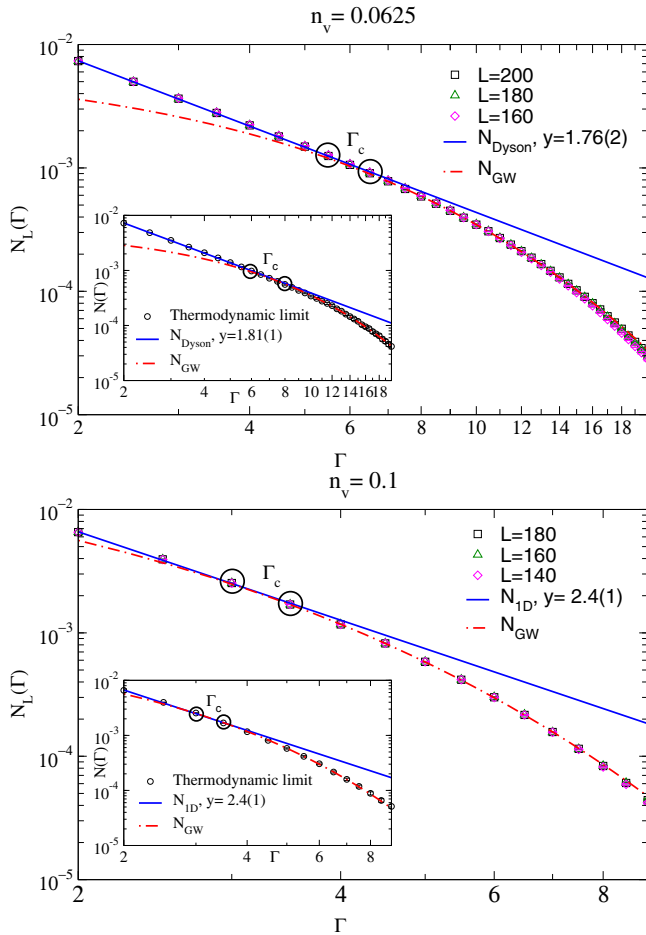
FIG. 3. $N_L(\Gamma)$ at the three largest values of L studied for $n_v = 0.0625$ and $n_v = 0.1$. Insets show $N(\Gamma)$ obtained by extrapolation to the thermodynamic limit. Circles demarcate the crossover region centered at the crossover scale Γ_c. Data for $\Gamma \lesssim \Gamma_c$ fits well to power-law form $N_{\text{Dyson}}(\Gamma)$ with the values of y indicated in each case, while the large-Γ regime fits well to the modified Gade-Wegner form $N_{\text{GW}}(\Gamma)$.

visible at $n_v = 0.05$ and $n_v = 0.075$. From Fig. 4, we see that y decreases gradually with n_v, while Γ_c increases extremely rapidly as we go to smaller values of n_v, thereby limiting our ability to directly study this crossover for $n_v \lesssim 0.05$. However, one can nevertheless reliably compute the exponent y that characterizes the behavior of $\rho(\epsilon)$ in the intermediate regime $t \gg |\epsilon| \gg \epsilon_c$ (Fig. 5) and confirm that its value evolves smoothly (Fig. 4) down to these small values of n_v. This strongly suggests that the crossover identified by us is an intrinsic and generic feature of the density of states for any nonzero n_v.

The corresponding crossover length scale $l_c \equiv N(\Gamma_c)^{-1/2}$, which represents the mean spatial separation between nonzero-energy modes with $|\epsilon|/t < 10^{-\Gamma_c}$, grows relatively slowly (Fig. 6) as w is decreased, with $l_c \lesssim 50$ lattice units even at the smallest value of w studied (corresponding to $n_v = 0.05$). This explains why our extrapolations to the thermodynamic limit using finite-size
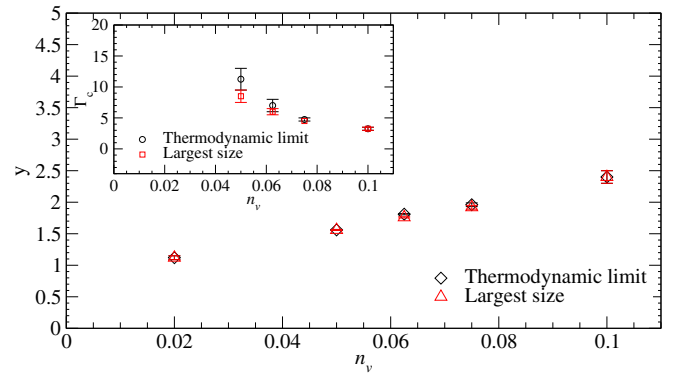

FIG. 4. n_v dependence of crossover scale Γ_c and power-law exponent y for samples with compensated random dilution.

data with $L \sim 200$ remain reliable for all n_v studied. From Fig. 6, which compares l_c for the randomly diluted samples with $l_w \equiv w^{-1/2}$, the mean spatial separation between zero modes, we also see that l_c tracks l_w (up to a nonuniversal prefactor). This suggests that the crossover identified in this Letter is controlled primarily by the density of zero modes. Additional support for this idea comes from our study of samples diluted with an equal number of randomly placed four-triangles (instead of individual vacancies) on each sublattice (see the Supplemental Material [34]), which show the same crossover, but with very different values of ϵ_c and y that are better predicted by the zero-mode density w as opposed to the vacancy density. This then leads us to the questions identified earlier: Is the physics of this crossover universally controlled by the value of w (i.e., independent of correlations between vacancy positions and other microscopic details) in the limit of small w, and can it be understood via a renormalization group description of the low-energy physics?
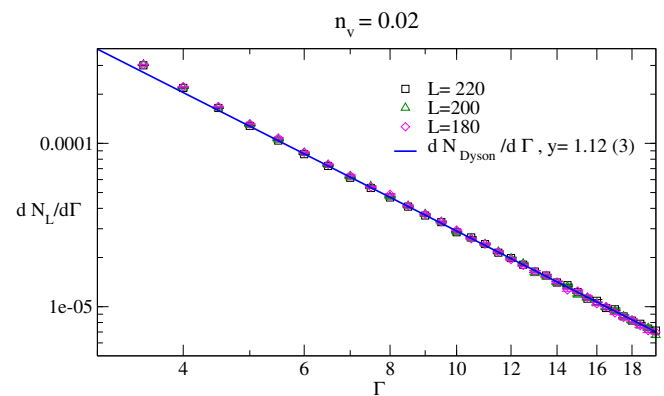

FIG. 5. $dN_L(\Gamma)/d\Gamma$ at $n_v = 0.02$ in the crossover regime converges to the thermodynamic limit for $L \sim 200$ and fits well to the form $dN_{\text{Dyson}}(\Gamma)/d\Gamma$, with a value of y consistent with the trends established at larger n_v for Γ_c and y (Fig. 4). Based on these trends, we expect $N(\Gamma)$ to cross over to the asymptotic form N_{GW} at much larger values of Γ, for which we are unable to reliably compute $N(\Gamma)$ due to computational constraints.
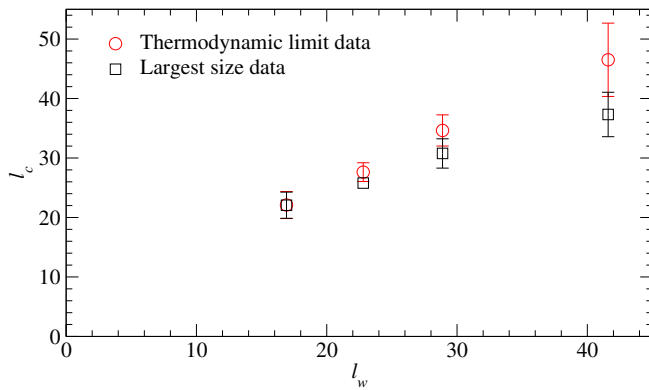
FIG. 6.   The crossover length scale $l_c \equiv N(\Gamma_c)^{-1/2}$ tracks the mean spatial separation $l_w \equiv w^{-1/2}$ between zero modes reasonably well for compensated random dilution. From left to right, the exhibited data points correspond to vacancy densities 0.1, 0.075, 0.0625, and 0.05.

[1] P. A. Lee and T. V. Ramakrishnan, Rev. Mod. Phys. **57**, 287 (1985).

[2] A. Altland, B. D. Simons, and M. R. Zirnbauer, Phys. Rep. **359**, 283 (2002).

[3] F. Evers and A. D. Mirlin, Rev. Mod. Phys. **80**, 1355 (2008).

[4] R. Gade, Nucl. Phys. **B398**, 499 (1993).

[5] R. Gade and F. Wegner, Nucl. Phys. **B360**, 213 (1991).

[6] O. I. Motrunich, K. Damle, and D. A. Huse, Phys. Rev. B **65**, 064206 (2002).

[7] P. T. Araujo, M. Terrones, and M. S. Dresselhaus, Mater. Today **15**, 98 (2012).

[8] G. Forte, A. Grassi, G. M. Lombardo, A. La Magna, G. G. N. Angilella, R. Pucci, and R. Vilardi, Phys. Lett. A **372**, 6168 (2008).

[9] V. M. Pereira, J. M. B. Lopes dos Santos, and A. H. Castro Neto, Phys. Rev. B **77**, 115109 (2008).

[10] V. M. Pereira, F. Guinea, J. M. B. Lopes dos Santos, N. M. R. Peres, and A. H. Castro Neto, Phys. Rev. Lett. **96**, 036801 (2006).

[11] T. O. Wehling, S. Yuan, A. I. Lichtenstein, A. K. Geim, and M. I. Katsnelson, Phys. Rev. Lett. **105**, 056802 (2010).

[12] F. J. Dyson, Phys. Rev. **92**, 1331 (1953).

[13] G. Theodorou and M. H. Cohen, Phys. Rev. B **13**, 4597 (1976).

[14] T. P. Eggarter and R. Riedinger, Phys. Rev. B **18**, 569 (1978).

[15] O. Motrunich, K. Damle, and D. A. Huse, Phys. Rev. B **63**, 134424 (2001).

[16] O. Motrunich, K. Damle, and D. A. Huse, Phys. Rev. B **63**, 224204 (2001).

[17] I. A. Gruzberg, N. Read, and S. Vishveshwara, Phys. Rev. B **71**, 245124 (2005).

[18] P. W. Brouwer, A. Furusaki, I. A. Gruzberg, and C. Mudry, Phys. Rev. Lett. **85**, 1064 (2000).

[19] P. W. Brouwer, C. Mudry, and A. Furusaki, Phys. Rev. Lett. **84**, 2913 (2000).

[20] M. Titov, P. W. Brouwer, A. Furusaki, and C. Mudry, Phys. Rev. B **63**, 235318 (2001).

[21] C. Mudry, S. Ryu, and A. Furusaki, Phys. Rev. B **67**, 064202 (2003).

[22] A. J. Willans, J. T. Chalker, and R. Moessner, Phys. Rev. B **84**, 115146 (2011).

[23] P. M. Ostrovsky, I. V. Protopopov, E. J. Konig, I. V. Gornyi, A. D. Mirlin, and M. A. Skvortsov, Phys. Rev. Lett. **113**, 186803 (2014).

[24] V. Hafner, J. Schindler, N. Weik, T. Mayer, S. Balakrishnan, R. Narayanan, S. Bera, and F. Evers, Phys. Rev. Lett. **113**, 186802 (2014).

[25] E. H. Lieb and M. Loss, Duke Math. J. **71**, 337 (1993).

[26] S. Ryu and Y. Hatsugai, Phys. Rev. Lett. **89**, 077002 (2002).

[27] L. Brey and H. A. Fertig, Phys. Rev. B **73**, 235411 (2006).

[28] P. W. Brouwer, E. Racine, A. Furusaki, Y. Hatsugai, Y. Morita, and C. Mudry, Phys. Rev. B **66**, 014204 (2002).

[29] https://en.wikipedia.org/wiki/ALGOL.

[30] R. S. Martin and J. H. Wilkinson, in *Handbook for Automatic Computation: Linear Algebra*, edited by J. H. Wilkinson and C. Reinsch (Springer-Verlag, Berlin, 1971), Vol. II.

[31] S. Sanyal, Ph.D. thesis, Tata Institute of Fundamental Research, Mumbai, 2014, http://theory.tifr.res.in/Research/Thesis/.

[32] https://en.wikipedia.org/wiki/GNU_Multiple_Precision_Arithmetic_Library.

[33] https://en.wikipedia.org/wiki/LAPACK.

[34] See Supplemental Material at http://link.aps.org/supplemental/10.1103/PhysRevLett.117.116806 for additional numerical and analytical evidence in support of our conclusions.